Isotopic (Cu, Zn, and Pb) and elemental fingerprints of antifouling paints and their potential use for environmental forensic investigations

Hyeryeong Jeong, Daniel Ferreira Araujo, Joël Knoery, Nicolas Briant, Kongtae Ra

Isotopic (Cu, Zn, and Pb) and elemental fingerprints of antifouling paints and their potential use for environmental forensic investigations

Hyeryeong Jeong[a,b,*], Daniel F. Araújo[a], Joël Knœry[a], Nicolas Briant[a], Kongtae Ra[b,c]

[a]Ifremer, CCEM-Unité Contamination Chimique des Ecosystèmes Marins (CCEM), F-44300 Nantes, France

[b]Marine Environmental Research Center, Korea Institute of Ocean Science and Technology (KIOST), Busan 49111, South Korea

[c]Department of Ocean Science (Oceanography), KIOST School, University of Science and Technology (UST), Daejeon 34113, South Korea

*Correspondence: hrjeong617@gmail.com

Abstract

Antifouling paints (APs) are one of the important sources of Cu and Zn contamination in coastal environments. This study applied for the first-time a multi-isotope (Cu, Zn, and Pb) and multi-elemental characterization of different AP brands to improve their tracking in marine environments. The Cu and Zn contents of APs were shown to be remarkably high ~35% and ~8%, respectively. The $\delta^{65}Cu_{AE647}$, $\delta^{66}Zn_{IRMM3702}$, and $^{206}Pb/^{207}Pb$ of the APs differed depending on the manufacturers and color (–0.16 to +0.36‰, –0.34 to +0.03‰, and 1.1158 to 1.2140, respectively). A PCA analysis indicates that APs, tires, and brake pads have also distinct elemental fingerprints. Combining isotopic and elemental ratios (e.g., Zn/Cu) allows to distinguish the environmental samples. Nevertheless, a first attempt to apply this approach in highly urbanized harbor areas demonstrates difficulties in source apportionments, because the sediment was chemically and isotopically homogeneous. The similarity of isotope ranges between the harbor and non-exhaust traffic emission sources suggests that most metals are highly affected by urban runoff, and that APs are not the main contributors of these metals. It is suspected that AP-borne contamination should be punctual rather than dispersed, because of APs low solubility properties. Nevertheless, this study shows that the common coastal anthropogenic sources display different elemental and isotopic fingerprints, hence the potential for isotope source tracking applications in marine environments. Further study cases, combined with laboratory experiments to investigate isotope fractionation during releasing the metal sources are necessary to improve non-traditional isotope applications in environmental forensics.

Keywords: Metal pollution, Hazard materials, Metal isotopes, Isotopic signatures, Harbor sediment, Tracing pollution sources

1. Introduction

The adhesion of biofouling marine organisms to submerged surfaces, such as marine leisure and shipping vessels, is a serious socioeconomic issue (Ytreberg et al., 2016; Davidson et al., 2021) as it is a major cause of an increase in ship drag penalty and hence in fuel consumption (Utama and Nugroho, 2018). Additionally, it can lead to high vessel maintenance costs, while the frequent need to clean the hull can shorten the dry-docking interval (Ytreberg et al., 2021). The annual costs to the global shipping industry of biofouling, including its prevention, increased fuel consumption, and vessel maintenance, are in the billions of Euros range (Desher, 2018; Whitworth et al., 2022).

After the worldwide ban on biocidal organotin compounds, such as tributyltin (TBT), in antifouling paints (APs), the tin-free alternatives have consisted largely of Cu(I)-based biocidal substances, such as cuprous oxide (Cu_2O) and copper thiocyanate (CuSCN), with zinc oxide (ZnO), and zinc pyrithione (ZnPT) as booster biocides (Turner, 2010; Muller-Karanassos et al., 2021). The high contents of these toxic metals in APs imply a risk of their release into the marine environment at variable rates that depend on the physical and chemical parameters of the aqueous medium.

Cu and Zn are essential micronutrients for living organisms, but at high concentrations, their bioaccumulation can result in considerable toxicity, with negative impacts on benthic ecosystems and marine organisms as well as degradation of water quality. For example, high Cu bioavailability was shown to damage the endocrine systems of oysters at the larval life stage (Gamain et al., 2017; Mai et al., 2012; Sussarellu et al., 2018; Wang et al., 2018; Wijsman et al., 2019).

Lead (Pb) compounds are also used in marine paints, due to their corrosion resistance, rapid curing, color, and opacity (Turner, 2014). Nonetheless, their harmful effects on human health (Turner, 2014), have led to the establishment in many countries of the following threshold values of Pb addition to paints: USA, Canada, Philippines, Nepal; 90 ppm, Switzerland, Thailand; 100 ppm, Brazil, the Republic of Korea, Argentina, Mexico; 600 ppm, New Zealand, Australia; 1000 ppm, as well as various countries have Pb restrictions on paints (UNEP, 2016). Furthermore, paint peelings from abandoned boats contained considerably high concentrations of Pb, Zn, and Cu (Rees et al., 2014), and may thus contaminate local sediments, transforming them into legacy pollution sources in marine environments. Major environmental and health

risks for the biota and for humans may also arise from speciation changes during post-depositional processes in sediments, which modify the bioavailability and toxicity of these metals, especially Pb (Rees et al., 2014). Because the aquatic environment gradually leaches APs from treated surfaces, AP efficiency decreases over time, requiring to periodically renew them (Soroldoni et al., 2018). The dissolved components and particles in the APs can be disseminated into the local environment (e.g., harbors, shipyards, and marinas), as also occurs when old AP coatings are removed, such as during vessel repair, maintenance, repainting, and cleaning (Turner et al., 2009; Soroldoni et al., 2017; 2018). Once in the marine environment, AP particles undergo various hydrodynamic processes (e.g., deposition, resuspension and dredging, dissolution, advection, and ultimately burial) (Turner, 2010). The release of biocidal as a result of biogeochemical and physiochemical reactions can adversely affect the marine biota and benthic ecosystems (Jones and Turner, 2010; Lagerström et al., 2016; Soroldoni et al., 2020).

The behavior of metals released from APs under variable physicochemical conditions has been evaluated extensively, mostly for the purpose of implementing environmental regulatory policies regarding AP use (Turner et al., 2009; Turner, 2010, 2014; Ytreberg et al., 2016, 2021; Soroldoni et al., 2017, 2018, 2020). However, accurate metal-based quantification of AP fluxes in the coastal environment remains challenging, since other anthropogenic metal sources are often impossible to deconvolve with traditional elemental analysis. Over the last 15 years, the development of techniques based on metal stable isotopes, including the quantification of metals and the discrimination of their sources, has opened up new perspectives in environmental forensics (Weiss et al., 2008; Bartelink et al., 2019; Pontér et al., 2021).

Isotopic fingerprints using radiogenic and stable isotope systems are advantageous techniques to track contaminants and source identification (Cheng and Hu, 2010, Kumar et al., 2014; Bi et al., 2017; Wang et al., 2021; Chen et al., 2022). Pb isotopic compositions reflect geogenic origins and are unaltered by physiochemical fractionation during anthropic activities (Shiel et al., 2010; Longman et al., 2018). The radioactive decays of thorium (Th) and uranium (U) induce different Pb isotopic compositions, and ^{208}Pb, ^{207}Pb, and ^{206}Pb are radioactive decay products of ^{232}Th, ^{235}U, and ^{238}U, respectively (Komárek et al., 2008). Distinct Pb isotopic ratios characterize in various geochemical reservoirs, and geogenic origins are more radiogenic than anthropogenic sources (Sangster et al., 2000; Knowlton and Moran, 2010; Zhu et al., 2013;

Kelepertzis et al., 2020; Liang et al., 2021). Diverse environmental reactions can lead to Cu and Zn isotopic fractionation in the interconnected earth systems (e.g., biosphere, hydrosphere, atmosphere, and lithosphere) (Wang et al., 2017; Souto-Oliveira et al., 2018; Köbberich and Vance, 2019; Liu et al., 2019; Liu et al., 2021; Araújo et al., 2022a). In general, adsorption of Cu and Zn to oxides (Pokrovsky et al., 2008; Bryan et al., 2015), organic matter (Jouvin et al., 2009; Araújo et al., 2022b), and soils (Bigalke et al., 2010) tends to preferentially enrich the heavy isotope on the surfaces (Guinoiseau et al., 2018), with rare exceptions (kaolinite; Li et al., 2015). The isotope systems of Zn, Cu, and Pb have been successfully used to track anthropogenic contamination in marine environments impacted by metallurgic (Yin et al., 2016; Tonhá et al., 2021; Yu et al., 2021), agricultural (Peng et al., 2020; Chen et al., 2022), and urban emissions (Gonzalez et al., 2016; Nazarpour et al., 2019). Thus far, only one study has investigated the use of Cu isotopes to trace AP contamination in sedimentary archives (Briant et al., 2022). Combining different isotope systems would allow source discrimination with improved resolution, as demonstrated in investigations of atmospheric pollution in urban aerosols (Souto-Oliveira et al., 2018; 2019; Schleicher et al., 2020). However, few studies have examined the applicability of this approach to marine systems, although they are often the ultimate repository for land-originating metal release.

Estuaries frequently receive anthropogenic effluents, including urban, industrial, and food production (agriculture, aquafarming, and fishing) activities (Araújo et al., 2019; Briant et al., 2021; Nel et al., 2022). Urban emissions are the dominant source of metal contamination in local aquatic environments, and they can distinctly affect the water quality (Deycard et al., 2014). Most coastal cities are densely populated, and many are geographically advantaged by their proximity to the mouths of large rivers (Wijesiri et al., 2019). However, adjacent maritime environments are thus more vulnerable to the deleterious effects of uncontrolled stormwater discharges (Jeong et al., 2020; Buzzi et al., 2022). Strongly urbanized estuaries tend to be susceptible to increased fluxes of metal-based compounds released from cities and urban structures (Deycard et al., 2014), such as non-exhaust traffic emission sources (e.g., wear of brake pads, tires, road paints, and road pavement) (Adamiec et al., 2016; Piscitello et al., 2021; Jeong et al., 2022). This multi-source road dust is transported together with surface soils into water systems vis stormwater runoff (Loganathan et al., 2013; Hwang et al., 2016; Wang et al., 2019).

The present study provides for the first time a multi-isotopic (Cu, Zn, and Pb) characterization in commercial APs. The isotopic fingerprints of APs are compared with other metal contamination sources including non-exhaust traffic emission sources. Furthermore, harbor sediment from a Korean marina is used to identify the potential useability of these isotopic and elemental fingerprints in a real-world environment.

2. Materials and methods

2.1. Anthropogenic source sampling

2.1.1 Antifouling paints

The 25 APs examined in this study are those generally used in Korea. The 11 domestic (Korean) APs were purchased from 5 different manufacturers (A, B, C, D, E). These were compared with 14 APs imported from different counties and produced by 4 manufacturers (F, G, H, I). Together, these 25 paints represent > 80% of the APs used in Korea. A 1- to 2-mm-thick layer of each AP was painted onto a Teflon sheet, which was then dried completely by placement on a 60 ℃ hot plate for several days.

2.1.2. Road dust, tire wear, and brake pads

Published data on road dust and particles from tire and brake pad wear were used for comparisons with potential sources in the estuarine environment. Road dust (25 samples) was vacuumed from an area of ~0.25 m^2 in Busan Metropolitan City. Brake pad and tire samples (from brands accounting for the majority of Korean market share) were broken up or cut into small pieces for homogenization and total digestion (Jeong et al., 2022; Jeong, 2022). Details of the sampling processes can be found in Jeong and Ra (2021), Jeong et al. (2022), and Jeong (2022).

2.2. Harbor sediments

Busan is the largest port city in Korea and the 6th largest container port in the world (WSC, 2019). Among Korean ports, it has the highest total traffic volume, largely due to the high

density of trans-shipment and ship repair facilities. Based on a previous study (Jeong et al., 2020), seven sampling sites were selected and the harbor sediments were collected using a grab-sampler in February 2020 (Fig. S1). The collected sediments were freeze-dried, homogenized, and stored in pre-acid cleaned PE bottles until the metal concentration and isotope measurements.

2.3. Sample preparation and elemental analysis

The dried APs were cut into small pieces and aliquots of ~50 mg were digested in Savillex digestion vessels. In the first step of the digestion procedure, high-purity nitric acid (HNO_3, Ultra-100, Kanto Chemical Co., Japan) was added, followed by evaporation of the samples to near dryness on a hot plate at 180 ℃; this step was then repeated. In the second step, the samples were treated with a mixed acid solution ($HF:HNO_3:HClO_4$ = 4:3:1; v/v) to achieve total digestion (Jeong et al., 2022), followed by evaporation as described above. The samples were then redissolved using 2% HNO_3. The same procedure was used to digest 50 mg amounts of the harbor sediment. All samples were prepared in duplicate. Metals were analyzed using an inductively coupled plasma mass spectrometer (ICP-MS; iCAP-Q, Thermo Scientific Co., Germany). All pre-treatment steps and analysis were performed in a clean room. The analytical quality of the metal analysis was confirmed by decomposing two certified reference materials (CRMs), MESS-4 and BCR-667, together with the environmental samples. The experimental concentrations obtained for CRMs were within ±10% of their certified values.

2.4. Metal stable isotope (Cu, Zn, and Pb) chromatography and analysis

Prior to measurements of the isotopic composition of Cu and Zn in APs and harbor sediments, the Cu and Zn digests were separated and purified on a 1 mL Teflon column (3.2 mm ID × 4.7 mm OD, Savillex, USA) filled with a Bio-Rad AG-MP1 anion exchange resin (analytical grade, 100–200 mesh, USA). The retained matrix was removed by the addition of 5 mL, and the Cu fraction by subsequent elution with 19 mL 7 mol/L HCl + 0.001% H_2O_2. The Fe fraction was removed using 16 mL 1 mol/L HCl + 0.001% H_2O_2. Finally, the Zn fraction was eluted in 10 mL 0.5 mol/L HNO_3. Cu was obtained on a second column to avoid element interference. The column separation protocols are described in detail in Jeong et al. (2021). In some paint samples,

high concentrations of Ti and Ba interferents remained in the purified fractions even after two-step column separation. Therefore, the Cu samples were purified on a third column using the same protocol described for the second column. For the Pb isotope analyses, Pb was purified using a 2 mL Eichrom column with a Pb-specific resin (100–150 μm particle size, Eichrom, France) (Jeong et al., 2021).

For precise isotope measurements, the standard-sample bracketing method and instrumental mass bias correction method were adopted by spiking Zn for Cu isotopes (and vice versa) and Tl for Pb isotopes. The average uncertainty (2sd) in duplicate samples was ±0.05‰ for $\delta^{65}Cu_{AE647}$, ±0.02‰ for $\delta^{66}Zn_{IRMM3702}$, and ±0.0002 for the $^{206}Pb/^{207}Pb$ ratio. The isotope analyses were conducted in samples containing 100 μg/L for Cu, 200 μg/L for Zn, and 50 μg/L for Pb. The Cu, Zn, and Pb isotopic compositions were measured using a multi-collector ICP-MS (MC-ICP-MS, Neptune Plus, Thermo Scientific Co., Germany) at the Korea Institute of Ocean Science and Technology (KIOST).

In-house standard solutions were used for quality control to ensure the accuracy of the isotope measurements. ERM-AE633 and Kanto Cu solution were used for the determination of Cu, yielding average $\delta^{65}Cu_{AE647}$ values of –0.21 ± 0.03‰ (2sd, n = 8) and +0.12 ± 0.01‰ (2sd, n = 8), respectively. IRMM-651 and Kanto Zn solution were used for the determination of Zn, yielding average $\delta^{66}Zn_{IRMM3702}$ values of –11.59 ± 0.01‰ (2sd, n = 4) and –0.07 ± 0.02‰ (2sd, n = 5) respectively. The average values for $\delta^{65}Cu_{AE647}$ and $\delta^{66}Zn_{IRMM3702}$ obtained using BHVO-2 were –0.08 ± 0.03‰ (2sd, n = 3) and –0.05 ± 0.09‰ (2sd, n = 3), respectively; these values were within the range of previously reported values (Sossi et al., 2015; Wang et al., 2020; Jeong et al., 2021) (Table 1).

The isotopic compositions of Cu and Zn are expressed in δ notation as the per mil (‰) deviation from the reference material:

$$\delta^{65}Cu\ (‰) = \left(\frac{(^{65}Cu/^{63}Cu)_{sample}}{(^{65}Cu/^{63}Cu)_{ERM-AE647}} - 1\right) \times 1000$$

$$\delta^{66}Zn\ (‰) = \left(\frac{(^{66}Zn/^{64}Zn)_{sample}}{(^{66}Zn/^{64}Zn)_{IRMM-3702}} - 1\right) \times 1000$$

Cu and Zn isotopic values were converted as follows to compare with previously reported values (Moeller et al., 2012; Araújo et al., 2017):

$$\delta^{65}Cu_{ERM-AE647} = \delta^{65}Cu_{NIST976} - 0.21‰$$

$$\delta^{66}Zn_{IRMM3702} = \delta^{66}Zn_{JMC} - 0.27‰$$

For Pb isotopes, the relative ratios of four stable isotopes (^{204}Pb, ^{206}Pb, ^{207}Pb, and ^{208}Pb) are reported.

2.5. Enrichment factor calculation

The enrichment factor (EF) is commonly used to assess the anthropogenic impact of metal contamination in sediments, and to classify contamination levels. It is calculated as follows (Ra et al., 2014):

$$\mathrm{EF} = \frac{\left(metal/_{Al}\right)_{sample}}{\left(metal/_{Al}\right)_{background}}$$

where metal/Al_{sample} and metal/$Al_{background}$ are the ratios of sediment and continental crust (Rudnick and Gao, 2003), respectively.

2.6. Principal component analysis

Principal component analysis (PCA) is used to recombine variables in multivariate data, with most of the variance explained by the first few variables (Xue et al., 2011). In this study, PCA was performed to identify the intercorrelations of potential sources of metal contamination (i.e., APs, brake pads, tires, and road dust) using PASW Statistics version 18. Eigenvalues > 1 were extracted for the first two components. To improve the accuracy of the results, the variables were varimax rotated.

3. Results and discussion

3.1. Elemental and isotope compositions of anthropogenic sources

3.1.1 Antifouling paints

Overall, the mean metal concentrations in domestic APs ranked as follows: Cu (30.46%) > Zn (6.58%) > Fe (1.97%) > Ti (1.64%) > Al (0.24%) > Sn (374.8 mg/kg) > Pb (143.4 mg/kg) > Ni (83.0 mg/kg) > Cr (51.7 mg/kg) > Mn (46.8 mg/kg) > Sb (5.61 mg/kg) > Mo (3.58 mg/kg) > V (3.15 mg/kg) > As (2.69 mg/kg) > Co (2.16 mg/kg) > Cd (0.93 mg/kg). Domestic APs had higher concentrations of Fe, Mn, V, Cr, Co, Sn, and Sb compared with imported APs (Table 2). The concentrations of Al, Ni, and Mo were similar between domestic and imported APs, while the concentrations of of Cu, Zn, As, Cd, and Pb were slightly higher in imported than domestic APs. The metal composition of APs produced by the same manufacturer varied depending on the paint color, with white APs having a higher Ti concentration (8.97%), but lower concentrations of other elements compared with blue, red, and black paints (Table S1). The concentrations of many metals (Cr, Ni, Cu, Zn, Cd, Sn, and Pb) were higher in APs than in either road paint (Jeong et al., 2022) or car paint (Hsu et al., 2018). Our data are consistent with other studies in which even higher Cu and Zn concentrations in APs were reported. Nevertheless, the Cu, Zn, and Pb concentrations in the APs differed by 3-, 1700-, and 26-fold, respectively, depending on the manufacturer.

The isotopic compositions of Cu, Zn, and Pb in domestic and imported APs are shown in Table 3. The Cu concentration in all APs ranged widely, from 17.33% to 52.12% (Fig. 1a); $\delta^{65}Cu_{AE647}$ values ranged from –0.16 to +0.36‰, except for two outliers (AP-H and AP-G, Table 3), with most of APs falling within a narrow isotope range of +0.18 to +0.36‰, close to that previously reported for these products (mean $\delta^{65}Cu_{AE647}$: +0.33‰ ± 0.10, 2sd, n = 3; Briant et al., 2022). The $^{206}Pb/^{207}Pb$ ratio in domestic APs was overall homogenous, ranging from 1.17 (AP-B) to 1.20 (AP-C), with an average of 1.1829 ± 0.0267 (2sd, n = 11). The average $^{206}Pb/^{207}Pb$ ratio in imported APs was 1.1870 ± 0.0559 (2sd, n = 14), which was similar to that in domestic APs (Fig. 1b). Sample AP-H was an outlier with respect to the isotopic values of Cu and Pb (Table 3). The Zn isotopic composition ($\delta^{66}Zn_{IRMM3702}$) showed a variability of approximately 0.4‰ and the mean $\delta^{66}Zn_{IRMM3702}$ value of all APs was –0.10 ± 0.20‰ (2sd, n = 25). The Zn isotopic values were simailr between domestic (–0.11 ± 0.23‰; 2sd, n = 11) and imported products (–0.09 ± 0.18‰; 2sd, n = 14) (Fig. 1c). White APs had a lower Cu concentration and the lightest Cu isotopic value (mean: +0.09 ± 0.35‰; 2sd, n = 2) compared with those of other colors (blue, red, and blank) (Table S2). Blue APs had a relatively lighter Zn isotopic composition, while red APs had a distinct Pb isotopic composition compared with those of other colors.

3.1.2 Non-exhaust urban sources: road dust, tire, and brake pads

Urban sources were adopted to compare with different potential sources as reported in previous studies. Non-exhaust traffic emission sources (e.g., wear of brake pads, tires, road paints, road pavement, and railway) are major sources of metal contamination in urban environments (Adamiec et al., 2016; Piscitello et al., 2021; Jeong et al., 2022). Road dust, brake pads, and tires were considered dominant urban sources in this study. Isotopic compositions of road dust in Busan were +0.05 ± 0.09‰, (2sd, n = 25; $\delta^{65}Cu_{AE647}$), –0.11 ± 0.06‰ (2sd, n = 25; $\delta^{66}Zn_{IRMM3702}$), and 1.1514 ± 0.0073 (2sd, n = 25, $^{206}Pb/^{207}Pb$) (Jeong and Ra, 2021). The isotopic values of particles from Korean tires were –0.51 ± 0.31‰ (2sd, n = 12; $\delta^{65}Cu_{AE647}$), –0.06 ± 0.05‰ (2sd, n = 12; $\delta^{66}Zn_{IRMM3702}$), and 1.1568 ± 0.0294 (2sd, n = 12; $^{206}Pb/^{207}Pb$) (Jeong, 2022). The $\delta^{65}Cu_{AE647}$, $\delta^{66}Zn_{IRMM3702}$, and $^{206}Pb/^{207}Pb$ values in particles from Korean brake pads were +0.18 ± 0.04‰ (2sd, n = 9), –0.04 ± 0.06‰ (2sd, n = 9), and 1.2645 ± 0.2865 (2sd, n = 9), respectively (Jeong et al., 2022). Excluding a single high Pb isotopic ratio ($^{206}Pb/^{207}Pb$) of brake pads, the average is 1.2199 ± 0.1010 (2sd, n = 8).

3.2. Harbor sediments

The mean metal concentrations in harbor sediments (Table 2) decreased in the order Zn > Cu > V > Cr > Pb > Ni > Co > As > Sn > Mo > Sb > Cd. Notably, the Cu concentration in coastal sediment outside of harbor area (35.6 mg/kg, Jeong et al., 2020) was 5.5 times lower than that measured in the harbor sediment in this study.

At site H7, the Cu concentration was 282.4 mg/kg, and thus higher than that of Zn (238.2 mg/kg). The mean $\delta^{65}Cu_{AE647}$ and $\delta^{66}Zn_{IRMM3702}$ values in harbor sediments were +0.06 ± 0.08‰ (2sd, n = 7) and –0.11 ± 0.07 ‰ (2sd, n = 7), respectively. The mean Pb isotopic ratio ($^{206}Pb/^{207}Pb$) was 1.1694 ± 0.0079 (2sd, n = 7), with a range of 1.1630 to 1.1733.

Among metals, Cu had the highest mean EF (7.2), ranging from 4.1 to 11.0, indicative of moderate to significant Cu contamination. The mean EF in harbor sediments decreased as follows: Cu > Zn > Cd > Pb > Sn > Sb > As > Mo > V > Cr > Co > Ni. Cu contamination was higher than Zn contamination, indicating anthropogenic Cu sources from harbor activities. In

301 the drainage basin of the study area, there is a high volume of vessel traffic in addition to many
302 ship repair facilities along its coastline.

303

304 *3.3. Source discrimination and comparison of isotopic and elemental fingerprints from coastal*
305 *anthropogenic sources*

306 The elemental and isotope information described for anthropogenic sources in previous
307 sections are used here to examine whether the isotopic and elemental fingerprints can be used
308 for source discrimination in the marine environment. To trace the sources of observed elevated
309 a PCA yield two principal components explaining > 80% (PC1 65% and PC2 20%), (Fig. 2).
310 PC1 had a strongly positive correlation with road dust and brake pads, and PC2 indicated a
311 significantly positive correlation with tires. The differences in clusters according to specific
312 anthropic material as determined in the PCA enabled the differentiation of these sources in the
313 coastal environment (Fig. 2). The isotopic and elemental proxies of these sources and their use
314 in tracking their potential contributions on harbor sediment are described below.

315 Elemental ratios are also widely used as a proxy for metal sources (Abbasi et al., 2021; Hong
316 et al., 2018; Wu and Huang, 2021; Zhang et al., 2014). For example, Zn/Cu and Cu/Sb have
317 been successfully applied to discriminate among traffic-activity-related sources in urban
318 environments (Iijima et al. 2007; Hwang et al., 2016; Jeong et al., 2020; McKenzie et al., 2009).
319 As noted above, anthropic materials can be discriminated according to their chemical
320 composition, and specifically by their different relative contents of Cu and Zn. Therefore, the
321 Zn/Cu ratio may be used to estimate potential sources of metal contamination in harbor
322 sediments. Figure 3 shows the relationship between the Zn/Cu ratio and the isotopic
323 compositions of Cu, Zn, and Pb. The mean Zn/Cu ratio of harbor sediment in this study was
324 1.6 (range: 0.8–2.6). This was slightly higher than the mean Zn/Cu ratio of APs and lower than
325 the Zn/Cu ratio of soil and road dust. Brake pads and APs with extremely high Cu
326 concentrations 47.3% and 36.0%, respectively, had similar Cu isotopic compositions. However,
327 the Zn/Cu ratio of brake pads was lower than that of APs, indicating that these two sources can
328 be distinguished (Fig. 3a). As shown in Fig. 3b, anthropogenic Zn tended to have an isotopically
329 light composition, and its elemental ratio (Zn/Cu) enable to discriminate among the different
330 sources (APs, road dust, brake pads, tires, and background soils). By contrast, it is difficult to
331 find distinct characteristics of potential sources using Pb isotopic ratios ($^{206}Pb/^{207}Pb$) due to

their homogeneity (Fig. 3c). Considering the Cu and Zn contamination levels in harbor sediments, the contribution of road dust to the estuarine environment is likely to be greater than that of APs. The result of this study also showed that Cu contamination in harbor sediments was affected by road dust, soil, and APs, simultaneously.

3.4. Metal isotope tracking in a Korean harbor

The relationships between the isotopic compositions of Cu, Zn, and Pb in harbor sediments and those of other potential sources, including APs, are shown in Fig. 4. The mean of $\delta^{65}Cu_{AE647}$ values was lower in harbor sediments than in domestic APs (+0.27‰, Table 3). The Zn isotopic composition was similar between the harbor sediments and APs, whereas the Pb isotopic ratio ($^{206}Pb/^{207}Pb$) was lower in harbor sediments. The mean $\delta^{65}Cu_{AE647}$ and $\delta^{66}Zn_{IRMM3702}$ were similar between harbor sediments and road dust (Jeong and Ra, 2021) (Fig. 4a). Cu and Zn isotopes in harbor sediments quite differed from those in non-exhaust emission sources in Korea, such as tire (Jeong, 2022) and brake pads (Jeong et al., 2022). Figure 4b shows the relationship between $^{206}Pb/^{207}Pb$ and $\delta^{66}Zn_{IRMM3702}$ values. The $\delta^{66}Zn_{IRMM3702}$ values in harbor sediments were similar to those in road dust and APs. The mean of $^{206}Pb/^{207}Pb$ values in harbor sediments was 1.1690, which was within the range of 1.1488 (road dust) and 1.1809 (APs). However, the isotopic composition of Zn and Pb in harbor sediments strongly differed from that in uncontaminated background soil ($\delta^{66}Zn_{IRMM3702}$: +0.10 ± 0.10‰, 2sd, n=6 and $^{206}Pb/^{207}Pb$: 1.1827 ± 0.0043, 2sd, n=6; Jeong and Ra, 2021). In the $^{206}Pb/^{207}Pb$ vs. $\delta^{65}Cu_{AE647}$ plot, the harbor sediment may have been affected by both geogenic (background soil) and anthropogenic (APs and road dust) sources (Fig. 4c). The isotopic compositions suggest that harbor sediments are not solely affected by APs, and that several other environmental sources affect surface sediments simultaneously.

Cu and Zn isotope mixing models have been successfully used to quantify source contributions in several pollution contexts: soils (Wang et al., 2021; Wang et al., 2022), sediments (Araújo et al., 2019; Nitzsche et al., 2022), water (Chen et al., 2008), and aerosols (Souto-Oliveira et al., 2018). It has been demonstrated that sources tend to be recorded almost conservatively in natural archives. This study shows that isotope fractionation during transport and post-deposition processes is not significant enough to obscure the source record. This should be related to small fractionation related in releasing of Cu and Zn by these materials. Briant et al.

(2022) reported similar Cu isotopic signatures between underlying sediment and APs ($\delta^{65}Cu_{NIST976}$: +0.44‰ and +0.54‰, respectively). This small difference is consistent with experimental works about adsorption onto surfaces (Komárek et al., 2022). Understanding the specific isotopic fractionation of each material is out of this present scope, but it remains an important step for advancing environmental forensic applications using isotopic tools in marine environments.

Pb isotope ratios are unaffected by biogeochemical processes (Komárek et al., 2008) and therefore, they are conservative in terms of Pb source recording. In contrast, Cu and Zn isotope ratios can change along their biogeochemical cycling. After releasing Cu and Zn in the marine environment, they are partitioned into different phases or compartments. Cu isotopic fractionation can occur by preferential organic complexation and light Cu isotope scavenging to the particles (Little et al., 2018). Theoretically, substances with stronger bonds (shorter bond length) tend to be enriched in heavier isotopes in equilibrium (Schauble, 2004; Wiederhold, 2015; Gou et al., 2018). In terms of sorption on mineral surfaces, Zn isotopic fractionation can be related to the ionic strength of the suspension, aqueous speciation, and molecular coordination environment (Veeramani et al., 2015). Moreover, isotopic fractionation can be affected by kinetics, isotope equilibrium effects, and many aspects of environmental processes (e.g., physical, chemical, and biological processes) (Cloquet et al., 2008; Desaulty and Petelet-Giraud, 2020).

Potential isotope fractionation during the transport of different environmental compartments remains uncertainty in the Cu isotope systems (Araújo et al., 2021). Cu and Zn isotope ratios behave conservatively in particulate phases during transport and post-depositional processes. This has been confirmed in highly dynamic environments like mangroves (Araújo et al., 2018), and the largest water flux river confluence in the world (Guinoiseau et al., 2018). As well, isotope records of sources in atmospheric and soil particles seems not be also significantly changed (Schleicher et al., 2020; Wang et al., 2021). Isotope systematics of sediments, suspended particulate matters, aerosols, and soils profiles are well explained by mixing models. Although these isotopic shifts in biogeochemical process are relatively small, sediment can preserve its contamination record, and is pertinent for source identification (Thapalia et al., 2010; 2015; Pontér et al., 2021). Nevertheless, these results show that the consideration of various environmental factors (size, shape, and density of AP particles) is needed for future

394 research, since these particles can be involved in mobility into the estuarine environments
395 (Soroldoni et al., 2018).

396

397 **Conclusions**

398 The establishment of databases on elemental and metal isotopes from anthropogenic sources is
399 a prerequisite for source apportionment studies in the field of environmental forensics. This
400 work provides the first multi-isotope and elemental characterization of APs. These materials
401 contain extremely high levels of Cu and Zn, and their progressive dispersion in the marine
402 environment leads to the release of these toxic metals, with damage to marine ecosystems. The
403 mean Cu ($\delta^{65}Cu_{AE647}$), Zn ($\delta^{66}Zn_{IRMM3702}$), and Pb ($^{206}Pb/^{207}Pb$) isotopic compositions of APs
404 were +0.22 ± 0.26‰ (2sd), −0.10 ± 0.20‰ (2sd), and 1.1852 ± 0.0448 (2sd), respectively.
405 While the concentrations of Cu, Zn, and Pb in APs differed widely depending on the
406 manufacturer, the isotopic compositions of the metals fell within a relatively narrow range,
407 with similar values for Korean-made and Korean-imported APs. Taken together, the elemental
408 and isotopic characterization of APs provided fingerprints that allowed them to be
409 distinguished from other sources (road dust, brake pads, and tires). These new data for APs
410 extend the isotope catalog for anthropic materials reported in the literature. It also demonstrated
411 that anthropogenic sources can be differentiated based on their chemical composition to track
412 contaminants in the coastal environment. The fingerprint of harbor sediment was close to that
413 of road dust. Because this study area is a densely populated port city and is highly influenced
414 by not only shipping but also urban (especially, traffic-related) activities. These results
415 demonstrate the feasibility of source identification using isotopic and elemental ratios in real-
416 world environments.

417

CRediT authorship contribution statement

Hyeryeong Jeong: Conceptualization, Investigation, Metal and Isotope analysis, Visualization, Validation, Writing-original draft. **Daniel F. Araújo:** Validation, Writing-Review & Editing. **Joël Knœry:** Validation, Writing-Review & Editing. **Nicolas Briant:** Validation, Writing-Review & Editing. **Kongtae Ra:** Methodology, Sampling, Metal and Isotope analysis, Visualization, Funding acquisition, Writing-Review & Editing.

Declaration of competing interest

The authors declare that they have no known competing financial interests that could have appeared to influence the work reported in this manuscript and have no conflicts of interest to declare that are relevant to this study.

Acknowledgements

This research was supported by a grant (PEA0023) from the Korea Institute of Ocean Science and Technology (KIOST): it was also supported by the "Development of source identification and apportionment methods for toxic substances in marine environments" program of the Korea Institute of Marine Science & Technology Promotion (KIMST) funded by the Ministry of Oceans and Fisheries (KIMST-20220534).

References

Abbasi, A., Salihoglu, I., Mirekhtiary, F., 2021. Trace element concentration and Al/Fe ratio in sediments of the South East Mediterranean Sea. Mar. Pollut. Bull. 171, 112788. https://doi.org/10.1016/j.marpolbul.2021.112788

Adamiec, E., Jarosz-Krzemińska, E., Wieszała, R., 2016. Heavy metals from non-exhaust vehicle emissions in urban and motorway road dusts. Environ. Monit. Assess. 188, 369. https://doi.org/10.1007/s10661-016-5377-1

Araújo, D.F., Boaventura, G.R., Viers, J., Mulholland, D.S., Weiss, D., Araujo, D., Lima, B., Ruiz, I., Machado, W., Babinski, M., Dantas, E., 2017. Ion exchange chromatography and mass bias correction for accurate and precise Zn isotope ratio measurements in environmental reference materials by MC-ICP-MS. J. Braz. Chem. Soc., 28, 225–235. https://doi.org/10.5935/0103-5053.20160167

Araújo, D.F., Machado, W., Weiss, D., Mulholland, D.S., Garnier, J., Souto-Oliveira, C.E., Babinski, M., 2018. Zinc isotopes as tracers of anthropogenic sources and biogeochemical processes in contaminated mangroves. Appl. Geochem. 95, 25–32. https://doi.org/10.1016/j.apgeochem.2018.05.008

Araújo, D.F., Ponzevera, E., Briant, N., Knoery, J., Sireau, T., Mojtahid, M., Metzger, E., Brach-Papa, C., 2019. Assessment of the metal contamination evolution in the Loire estuary using Cu and Zn stable isotopes and geochemical data in sediments. Mar. Pollut. Bull. 143, 12–23. https://doi.org/10.1016/j.marpolbul.2019.04.034

Araújo, D.F., Knoery, J., Briant, N., Ponzevera, E., Chouvelon, T., Auby, I., Yepez, S., Bruzac, S., Sireau, T., Pellouin-Grouhel, A., Akcha, F., 2021. Metal stable isotopes in transplanted oysters as a new tool for monitoring anthropogenic metal bioaccumulation in marine environments: The case for copper. Environ. Pollut. 290, 118012. https://doi.org/10.1016/j.envpol.2021.118012

Araújo, D.F., Knoery, J., Briant, N., Vigier, N., Ponzevera, E., 2022a. "Non-traditional" stable isotopes applied to the study of trace metal contaminants in anthropized marine environments. Mar. Pollut. Bull. 175, 113398. https://doi.org/10.1016/j.marpolbul.2022.113398

Araújo, D.F., Knoery, J., Briant, N., Ponzevera, E., Mulholland, D.S., Bruzac, S., Sireau, T.,

Chouvelon, T., Brach-Papa, C., 2022b. Cu and Zn stable isotopes in suspended particulate matter sub-fractions from the northern Bay of Biscay help identify biogenic and geogenic particle pools. Cont. Shelf Res. 244, 104791. https://doi.org/10.1016/j.csr.2022.104791

Bartelink, E.J., Chesson, L.A., 2019. Resent applications of isotope analysis to forensic anthropology. Forensic Sci. Res. 4 (1), 29–44. https://doi.org/10.1080/20961790.2018.1549527

Bi, X.Y., Li, Z.G., Wang, S.X., Zhang, L., Xu, R., Liu, J.L., Yang, H.M., Guo, M.Z., 2017. Lead isotopic compositions of selected coals, Pb/Zn ores and fuels in China and the application for source tracing. Environ. Sci. Technol. 51, 13502–13508. https://doi.org/10.1021/acs.est.7b04119

Bigalke, M., Weyer, S., Kobza, J., Wilcke, W., 2010. Stable Cu and Zn isotope ratios as tracers of sources and transport of Cu and Zn in contaminated soil. Geochim. Cosmochim. Acta 74, 6801–6813. https://doi.org/10.1016/j.gca.2010.08.044

Briant, N., Chiffoleau, J.F., Knoery, J., Araújo, D.F., Ponzevera, E., Crochet, S., Thomas, B., Brach-Papa, C., 2021. Seasonal trace metal distribution, partition and fluxes in the temperate macrotidal Loire Estuary (France). Estuar. Coast. Shelf Sci. 262, 107616. https://doi.org/10.1016/j.ecss.2021.107616

Briant, N., Freydier, R., Araùjo, D.F., Delpoux, S., Elbaz-Poulichet, F., 2022. Cu isotope records of Cu-based antifouling paints in sediment core profiles from the largest European Marina, The Port Camargue. Sci. Total Environ. 849, 157885. https://doi.org/10.1016/j.scitotenv.2022.157885

Bryan, A.L., Dong, S., Wilkes, E.B., Wasylenki, L.E., 2015. Zinc isotope fractionation during adsorption onto Mn oxyhydroxide at low and high ionic strength. Geochim. Cosmochim. Acta 157, 182–197. https://doi.org/10.1016/j.gca.2015.01.026

Buzzi, N.S., Menéndez, M.C., Truchet, D.M., Delgado, A.L., Fernández Severini, M.D., 2022. An overview on metal pollution on touristic sandy beaches: Is the COVID-19 pandemic an opportunity to improve coastal management? Mar. Pollut. Bull. 174, 113275. https://doi.org/10.1016/j.marpolbul.2021.113275

Chen, J.B., Gaillardet, J., Louvat, P., 2008. Zinc isotopes in the Seine River waters, France: A

probe of anthropogenic contamination. Environ. Sci. Technol. 42, 6494–6501. https://doi.org/10.1021/es800725z

Chen, Z., Ding, Y., Jiang, X., Duan, H., Ruan, X., Li, Z., Li, Y., 2022. Combination of UNMIX, PMF model and Pb-Zn-Cu isotopic compositions for quantitative source apportionment of heavy metals in suburban agricultural soils. Ecotoxicol. Environ. Saf. 234, 113369. https://doi.org/10.1016/j.ecoenv.2022.113369

Cheng, H., Hu, Y., 2010. Lead (Pb) isotopic fingerprinting and its applications in lead pollution studies in China: A review. Environ. Pollut. 158, 1134–1146. https://doi.org/10.1016/j.envpol.2009.12.028

Cloquet, C., Carignan, J., Lehmann, M.F., Vanhaecke, F., 2008. Variation in the isotopic composition of zinc in the natural environment and the use of zinc isotopes in biogeosciences: a review. Anal. Bioanal. Chem. 390, 451–463. https://doi.org/10.1007/s00216-007-1635-y

Davidson, I., Cahill, P., Hinz, A., Kluza, D., Scianni, C., Georgiades, E., 2021. A review of biofouling of ship's internal seawater systems. Front. Mar. Sci. 8, 761531. https://doi.org/10.3389/fmars.2021.761531

Desaulty, A.M., Petelet-Giraud, E., 2020. Zinc isotope composition as a tool for tracing sources and fate of metal contaminants in rivers. Sci. Total Environ. 728, 138599. https://doi.org/10.1016/j.scitotenv.2020.138599

Desher, A.A., 2018. Biofouling impacts on the environment and ship energy efficiency. World Maritime University Dissertations 617. Malmö, Sweden.

Deycard, V.N., Schäfer, J., Blanc, G., Coynel, A., Petit, J.C.J., Lanceleur, L., Dutruch, L., Bossy, C., Ventura, A., 2014. Contributions and potential impacts of seven priority substances (As, Cd, Cu, Cr, Ni, Pb, and Zn) to a major European Estuary (Gironde Estuary, France) from urban wastewater. Mar. Chem. 167, 123–134. https://doi.org/10.1016/j.marchem.2014.05.005

Gamain, P., Cachot, J., Gonzalez, P., Budzinski, H., Gourves, P.-Y., Morin, B., 2017. Do temporal and spatial parameters or lifestyle of the Pacific oyster *Crasssostrea gigas* affect pollutant bioaccumulation, offspring development, and tolerance to pollutants? Front. Mar. Sci. 4. https://doi.org/10.3389/fmars.2017.00058

Gonzalez, R.O., Strekopytov, S., Amato, F., Querol, X., Reche, C., Weiss, D., 2016. New

524 insights from zinc and copper isotopic compositions into the sources of atmospheric particulate
525 matter from two major European Cities. Environ. Sci. Technol. 50, 9816–9824.
526 https://doi.org/10.1021/acs.est.6b00863

527 Gou, W., Li, W., Ji, J., Li, W., 2018. Zinc isotope fractionation during sorption onto Al oxides:
528 Atomic level understanding from EXAFS. Environ. Sci. Technol. 52, 9087–9096.
529 https://doi.org/10.1021/acs.est.8b01414

530 Guinoiseau, D., Bouchez, J., Gélabert, A., Louvat, P., Moreira-Turcq, P., Filizola, N., Benedetti,
531 M.F., 2018. Fate of particulate copper and zinc isotopes at the Solimões-Negro river confluence,
532 Amazon Basin, Brazil. Chem. Geol. 489, 1–15. https://doi.org/10.1016/j.chemgeo.2018.05.004

533 Hong, N., Zhu, P., Liu, A., Zhao, X., Guan, Y., 2018. Using an innovative flag element ratio
534 approach to tracking potential sources of heavy metals on urban road surfaces. Environ. Pollut.
535 243(Part A), 410-417. https://doi.org/10.1016/j.envpol.2018.08.098

536 Hsu, D.J., Chung, S.H., Dong, J.F., Shih, H.C., Chang, H.B., Chien, Y.C., 2018. Water-based
537 automobile paints potentially reduce the exposure of refinish painters to toxic metals. Int. J.
538 Environ. Res. Public Health 15, 899. https://doi.org/10.3390/ijerph15050899

539 Hwang, H.M., Fiala, M.J., Park, D., Wade, T.L., 2016. Review of pollutants in urban road dust
540 and stormwater runoff: part 1. Heavy metals released from vehicles. International Journal of
541 Urban Science 20, 334-360. https://doi.org/10.1080/12265934.2016.1193041

542 Iijima, A., Sato, K., Yano, K., Tago, H., Kato, M., Kimura, H., Furuta, N., 2007. Particle size
543 and composition distribution analysis of automotive brake abrasion dusts for the evaluation of
544 antimony sources of airborne particulate matter. Atmos. Environ. 41, 4908-4919.
545 https://doi.org/10.1016/j.atmosenv.2007.02.005

546 Jeong, H., Choi, J.Y., Lim, J., Shim, W.J., Kim, Y.O., Ra, K., 2020. Characterization of the
547 contribution of road deposited sediments to the contamination of the close marine environment
548 with trace metals: Case of the port city of Busan (South Korea). Mar. Pollut. Bull. 161, 111717.
549 https://doi.org/10.1016/j.marpolbul.2020.111717

550 Jeong, H., Ra, K., Choi, J.Y., 2021. Copper, zinc, and lead isotopic delta values and isotope
551 ratios of various geological and biological reference materials. Geostand. Geoanal. Res. 45,
552 551-563. https://doi.org/10.1111/ggr.12379

553 Jeong, H., Ra, K., 2021. Characteristics of potentially toxic elements, risk assessment, and
554 isotopic compositions (Cu-Zn-Pb) in the PM_{10} fraction of road dust in Busan, South Korea.
555 Atmosphere 12, 1229. https://doi.org/10.3390/atmos12091229

556 Jeong, H., 2022. Toxic metal concentrations and Cu-Zn-Pb isotopic compositions in tires. J.
557 Anal. Sci. Technol. 13, 2. https://doi.org/10.1186/s40543-021-00312-3

558 Jeong, H., Ryu, J.S., Ra, K., 2022. Characteristics of potentially toxic elements and multi-
559 isotope signatures (Cu, Zn, Pb) in non-exhaust traffic emission sources. Environ. Pollut. 292,
560 118339. https://doi.org/10.1016/j.envpol.2021.118339

561 Jones, D.E., Turner, A., 2010. Bioaccessibility and mobilisation of copper and zinc in estuarine
562 sediment contaminated by antifouling paint particles. Estuar. Coast. Shelf Sci. 87, 399–404.
563 https://doi.org/10.1016/j.ecss.2010.01.018

564 Jouvin, D., Louvat, P., Juillot, F., Maréchal, C.N., Benedetti, M.F., 2009. Zinc isotopic
565 fractionation: why organic matters Environ. Sci. Technol. 43, 5747–5754,
566 https://doi.org/10.1021/es803012e

567 Kelepertzis, E., Argyraki, A., Chrastný, V., Botsou, F., Skordas, K., Komárek, M., Fouskas, A.,
568 2020. Metal(loid) and isotopic tracing of Pb in soils, road and house dusts from the industrial
569 area of Volos (central Greece). Sci. Total Environ. 725, 138300.
570 https://doi.org/10.1016/j.scitotenv.2020.138300

571 Knowlton, S.W., Moran, S.B., 2010. Stable Pb isotope ratios in aerosols, precipitation, and
572 size-fractionated particulate matter in the Gulf of Maine, Scotian Shelf, and Labrador Sea. Mar.
573 Pollut. Bull. 60, 984–989. https://doi.org/10.1016/j.marpolbul.2010.02.005

574 Komárek, M., Ettler, V., Chrastný, V., Mihaljevič, M., 2008. Lead isotopes in environmental
575 sciences: A review. Environ. Int. 34, 562–577. https://doi.org/10.1016/j.envint.2007.10.005

576 Komárek, M., Ratié, G., Vaňková, Z., Šípková, A., Chrastný, V., 2022. Metal isotope
577 complexation with environmentally relevant surfaces: Opening the isotope fractionation black
578 box. Crit. Rev. Environ. Sci. Technol. 52, 3573–3603.
579 https://doi.org/10.1080/10643389.2021.1955601

580 Köbberich, M., Vance, D., 2019. Zn isotope fractionation during uptake into marine
581 phytoplankton: Implications for oceanic zinc isotopes. Chem. Geol. 523, 154–161.

https://doi.org/10.1016/j.chemgeo.2019.04.004

Kumar, A., Abouchami, W., Galer, S.J.G., Garrison, V.H., Williams, E., Andreae, M.O., 2014. A radiogenic isotope tracer study of transatlantic dust transport from Africa to the Caribbean. Atmos. Environ. 82, 130–143. http://dx.doi.org/10.1016/j.atmosenv.2013.10.021

Lagerström, M., Norling, M., Eklund, B., 2016. Metal contamination at recreational boatyards linked to the use of antifouling paints—investigation of soil and sediment with a field portable XRF. Environ. Sci. Pollut. Res. 23, 10146–10157. https://doi.org/10.1007/s11356-016-6241-0

Li, D., Liu, S.-A., Li, S., 2015. Copper isotope fractionation during adsorption onto kaolinite: experimental approach and applications. Chem. Geol. 396, 74–82. https://doi.org/10.1016/j.chemgeo.2014.12.020

Liang, X., Wang, C., Song, Z., Yang, S., Bi, X., Li, Z., Li, P., 2021. Soil metal(loid)s pollution around a lead/zinc smelter and source apportionment using isotope fingerprints and receptor models. Appl. Geochem. 135, 105118. https://doi.org/10.1016/j.apgeochem.2021.105118

Little, S.H., Archer, C., Milne, A., Schlosser, C., Achterverg, E.P., Lohan, M.C., Vance, D., 2018. Paired dissolved and particulate phase Cu isotope distributions in the South Atlantic. Chem. Geol. 502, 29–43. https://doi.org/10.1016/j.chemgeo.2018.07.022

Liu, S.A., Liu, P.P., Lv, Y., Wang, Z.Z., Dai, J.G., 2019. Cu and Zn isotope fractionation during oceanic alteration: Implications for Oceanic Cu and Zn cycle. Geochim. Cosmochim. Acta 257, 191–205. https://doi.org/10.1016/j.gca.2019.04.026

Liu, S., Li, Y., Liu, J., Yang, Z., Liu, J., Shi, Y., 2021. Equilibrium Cu isotope fractionation in copper minerals: a first-principles study. Chem. Geol. 564, 120060. https://doi.org/10.1016/j.chemgeo.2021.120060

Loganathan, P., Vigneswaran, S., Kandasamy, J., 2013. Road-deposited sediment pollutants: A critical review of their characteristics, source apportionment, and management. Crit. Rev. Environ. Sci. Technol. 43, 1315–1348. https://doi.org/10.1080/10643389.2011.644222

Longman, J., Veres, D., Ersek, V., Phillips, D.L., Chauvel, C., Tamas, C.G., 2018. Quantitative assessment of Pb sources in isotopic mixtures using a Bayesian mixing model. Sci. Rep. 8, 6154. https://doi.org/10.1038/s41598-018-24474-0

610 Mai, H., Cachot, J., Brune, J., Geffard, O., Belles, A., Budzinski, H., Morin, B., 2012.
611 Embryotoxic and genotoxic effects of heavy metals and pesticides on early life stages of Pacific
612 oyster (*Crassostrea gigas*). Mar. Pollut. Bull. 64, 2663–2670.
613 https://doi.org/10.1016/j.marpolbul.2012.10.009

614 McKenzie, E.R., Money, J.E., Green, P.G., Young, T.M., 2009. Metals associated with
615 stormwater-relevant brake and tire samples. Sci. Total Environ. 407, 5855–5860.
616 https://doi.org/10.1016/j.scitotenv.2009.07.018

617 Moeller, K., Schoenberg, R., Pedersen, R.B., Weiss, D., and Dong, S., 2012. Calibration of the
618 new certified reference materials ERMAE633 and ERM-AE647 for copper and IRMM-3702
619 for zinc isotope amount ratio determinations. Geostand. Geoanal. Res. 36, 177–199.
620 https://doi.org/10.1111/j.1751-908X.2011.00153.x

621 Muller-Karanassos, C., Arundel, W., Lindeque, P.K., Vance, T., Turner, A., Cole, M., 2021.
622 Environmental concentrations of antifouling paint particles are toxic to sediment-dwelling
623 invertebrates. Environ. Pollut. 268, 115754. https://doi.org/10.1016/j.envpol.2020.115754

624 Nazarpour, A., Watts, M.J., Madhani, A., Elahi, S., 2019. Source, spatial distribution and
625 pollution assessment of Pb, Zn, Cu, and Pb, isotopes in urban soils of Ahvaz City, a semi-arid
626 metropolis in Southwest Iran. Sci. Rep. 9, 5349. https://doi.org/10.1038/s41598-019-41787-w

627 Nel, M.A., Rubidge, G., Adams, J.B., Human, L.R.D., 2022. Contributions of wetland plants
628 on metal accumulation in sediment. Sustainability 14, 3679.
629 https://doi.org/10.3390/su14063679

630 Nitzsche, K.N., Yoshimura, T., Ishikawa, N.F., Kajita, H., Kawahata, H., Ogawa, N.O., Suzuki,
631 K., Yokoyama, Y., Ohkouchi, N., 2022. Metal contamination in a sediment core from Osaka
632 Bay during the last 400 years. Prog. Earth Planet. Sci. 9, 58. https://doi.org/10.1186/s40645-
633 022-00517-z

634 Peng, M., Zhao, C., Ma, H., Yang, Z., Yang, K., Liu, F., Li, K., Yang, Z., Tang, S., Guo, F., Liu,
635 X., Cheng, H., 2020. Heavy metal and Pb isotopic compositions of soil and maize from a major
636 agricultural area in Northeast China: Contamination assessment and source apportionment. J.
637 Geochem. Explor. 208, 106403. https://doi.org/10.1016/j.gexplo.2019.106403

638 Piscitello, A., Bianco, C., Casasso, A., Sethi, R., 2021. Non-exhaust traffic emissions: Sources,

639 characterization, and mitigation measures. Sci. Total Environ. 766, 144440.
640 https://doi.org/10.1016/j.scitotenv.2020.144440

641 Pokrovsky, O.S., Viers, J., Emnova, E.E., Kompantseva, E.I., Freydier, R., 2008. Copper
642 isotope fractionation during its interaction with soil and aquatic microorganisms and metal
643 oxy(hydr)oxides: Possible structural control. Geochim. Cosmochim. Acta 72, 1742–1757.
644 https://doi.org/10.1016/j.gca.2008.01.018

645 Pontér, S., Sutliff-Johansson, S., Engström, E., Widerlund, A., Mäki, A., Rodushkina, K.,
646 Paulukat, C., Rodushkin, I., 2021. Evaluation of a multi-isotope approach as a complement to
647 concentration data within environmental forensics. Minerals 11, 37.
648 https://doi.org/10.3390/min11010037

649 Ra, K., Kim, J.K., Hong, S.H., Yim, U.H., Shim, W.J., Lee, S.Y., Kim, Y.O., Lim, J.S., Kim,
650 E.S., Kim, K.T., 2014. Assessment of pollution and ecological risk of heavy metals in the
651 surface sediments of Ulsan Bay, Korea. Ocean Sci. J. 49, 279-289.
652 https://doi.org/10.1007/s12601-014-0028-3

653 Rees, A.B., Turner, A., Comber, S., 2014. Metal contamination of sediment by paint peeling
654 from abandoned boats, with particular reference to lead. Sci. Total Environ. 494–495, 313–319.
655 https://doi.org/10.1016/j.scitotenv.2014.06.064

656 Rudnick, R.I., Gao, S., 2003. Composition of the continental crust. In: Rudnick, R.L. (Ed.),
657 The Crust, Elsvier, pp. 1-64. https://doi.org/10.1016/B0-08-043751-6/03016-4

658 Sangster, D.F., Ouitridge, P.M., Davis, W.J., 2000. Stable lead isotope characteristics of lead
659 ore deposits of environmental significance. Environ. Res. 8, 115–147.
660 https://doi.org/10.1139/a00-008

661 Schauble, E.A., 2004. Applying stable isotope fractionation theory to new systems. Rev.
662 Mineral. Geochem. 55, 65−111. https://doi.org/10.2138/gsrmg.55.1.65

663 Schleicher, N.J., Dong, S., Packman, H., Little, S.H., Gonzalez, R.O., Najorka, J., Sun, Y.,
664 Weiss, D.J., 2020. A global assessment of copper, zinc, and lead isotopes in mineral dust
665 sources and aerosols. Front. Earth Sci. 8, 167. https://doi.org/10.3389/feart.2020.00167

666 Shiel, A.E., Weis, D, Orians, K.J., 2010. Evaluation of zinc, cadmium and lead isotope
667 fractionation during smelting and refining. Sci. Total Environ. 408, 2357–2368.

https://doi.org/10.1016/j.scitotenv.2010.02.016

Soroldoni, S., Abreu, F., Castro, Í.B., Duarte, F.A., Pinho, G.L.L., 2017. Are antifouling paint particles a continuous source of toxic chemicals to the marine environment? J. Hazard. Mater. 330, 76–82. https://doi.org/10.1016/j.jhazmat.2017.02.001

Soroldoni, S., Castro, Í.B., Abreu, F., Duarte, F.A., Choueri, R.B., Möller, O.O. Jr., Fillmann, G., Pinho, G.L.L., 2018. Antifouling paint particles: Sources, occurrence, composition and dynamics. Water Res. 137, 47–56. https://doi.org/10.1016/j.watres.2018.02.064

Soroldoni, S., da Silva, S.V., Castro, Í.B., Martins C.M.G., Pinho, G.L.L., 2020. Antifouling paint particles cause toxicity to benthic organisms: Effects on two species with different feeding modes. Chemosphere 238, 124610. https://doi.org/10.1016/j.chemosphere.2019.124610

Sossi, P.A., Halverson, G.P., Nebel, O., Eggins, S.M., 2015. Combined separation of Cu, Fe and Zn from rock matrices and improved analytical protocols for stable isotope determination. Geostand. Geoanal. Res. 39, 129–149. https://doi.org/10.1111/j.1751-908X.2014.00298.x

Souto-Oliveira, C.E., Babinski, M., Araújo, D.F., Andrade, M.F., 2018. Multi-isotopic fingerprints (Pb, Zn, Cu) applied for urban aerosol source apportionment and discrimination. Sci. Total Environ. 626, 1350–1366. https://doi.org/10.1016/j.scitotenv.2018.01.192

Souto-Oliveira, C.E., Babinski, M., Araújo, D.F., Weiss, D.J., Ruiz, I.R., 2019. Multi-isotope approach of Pb, Cu and Zn in urban aerosols and anthropogenic sources improves tracing of the atmospheric pollutant sources in megacities. Atmos. Environ. 198, 427–437. https://doi.org/10.1016/j.atmosenv.2018.11.007

Sussarellu, R., Lebreton, M., Rouxel, J., Akcha, F., Rivière, G., 2018. Copper induces expression and methylation changes of early development genes in *Crassostrea gigas* embryos. Aquat. Toxicol. 196, 70–78. https://doi.org/10.1016/j.aquatox.2018.01.001

Thapalia, A., Borrok, D.M., Metre, P.C.V., Musgrove, M., Landa, E.R., 2010. Zn and Cu isotope as tracers of anthropogenic contamination in sediment core from an urban lake. Environ, Sci. Technol. 44, 1544–1550. https://doi.org/10.1021/es902933y

Thapalia, A., Borrok, D.M., Metre, P.C.V., Wilson, J., 2015. Zinc isotopic signatures in eight lake sediment cores from across the United States. Environ. Sci. Technol. 49, 132–140. https://doi.org/10.1021/es5036893

Tonhá, M.S., Araújo, D.F., Araújo, R., Cunha, B.C.A., Machado, W., Portela, J.F., Souza, J.P.R., Carvalho, H.K., Dantas, E.L., Roig, H.L., Seyler, P., Garnier, J., 2021. Trace metal dynamics in an industrialized Brazilian river: A combined application of Zn isotopes, geochemical partitioning, and multivariate statistics. J. Environ. Sci. 101, 313–325. https://doi.org/10.1016/j.jes.2020.08.027

Turner, A., Singh, N., Richards, J.P., 2009. Bioaccessibility of metals in soils and dusts contaminated by marine antifouling paint particles. Environ. Pollut. 157, 1526–1532. https://doi.org/10.1016/j.envpol.2009.01.008

Turner, A., 2010. Marine pollution from antifouling paint particles. Mar. Pollut. Bull. 60, 159–171. https://doi.org/10.1016/j.marpolbul.2009.12.004

Turner, A., 2014. Mobilisation and bioaccessibility of lead in paint from abandoned boats. Mar. Pollut. Bull. 89, 35–39. https://doi.org/10.1016/j.marpolbul.2014.10.038

United Nations Environment Programme (UNEP), 2016. Global Report on the Status of Legal Limits on Lead in Paint.

Utama, I.K.A.P., Nugroho, B., 2018. Biofouling, ship drag, and fuel consumption: A brief overview. J. Ocean Technol. 13 (2), 42–48.

Veeramani, H., Eagling, J., Jamieson-Hanes, J.H., Kong, L., Ptacek, C.J., Blowes, D.W., 2015. Zinc isotope fractionation as an indicator of geochemical attenuation processes. Environ. Sci. Technol. Lett. 2, 314–319. https://doi.org/10.1021/acs.estlett.5b00273

Wang, W.-X., Meng, J., Weng, N., 2018. Trace metals in oysters: molecular and cellular mechanisms and ecotoxicological impacts. Environ. Sci. Process Impacts 20, 892–912. https://doi.org/10.1039/C8EM00069G

Wang, Q., Zhang, Q., Dzakpasu, M., Chang, N., Wang, X., 2019. Transferral of HMs pollution from road-deposited sediments to stormwater runoff during transport processes. Front. Environ. Sci. Eng. 13, 13. https://doi.org/10.1007/s11783-019-1091-x

Wang, Q., Zhou, L., Little, S.H., Liu, J., Feng, L., Tong, S., 2020. The geochemical behavior of Cu and its isotopes in the Yangtze River. Sci. Total Environ. 728, 138428. https://doi.org/10.1016/j.scitotenv.2020.138428

Wang, L., Jin, Y., Weiss, D.J., Schleicher, N.J., Wilcke, W., Wu, L., Guo, Q., Chen, J., O'Connor, D., Hou, D., 2021. Possible application of stable isotope compositions for the identification of metal sources in soil. J. Hazard. Mater. 407, 124812. https://doi.org/10.1016/j.jhazmat.2020.124812

Wang, D., Zheng, L., Ren, M., Li, C., Dong, X., Wei, X., Zhou, W., Cui, J., 2022. Zinc in soil reflecting the intensive coal mining activities: Evidence from stable zinc isotopes analysis. Ecotoxicol. Environ. Saf. 239, 113669. https://doi.org/10.1016/j.ecoenv.2022.113669

Wang, Z., Chen, J., Zhang, T., 2017. Cu isotopic composition in surface environments and in biological systems: A critical review. Int. J. Environ. Res. Public Health 14, 538. https://doi.org/10.3390/ijerph14050538

Weiss, D.J., Rehkdmper, M., Schoenberg, R., McLaughlin, M., Kirby, J., Campbell, P.G.C., Arnold, T., Chapman, J., Peel, K., Gioia, S., 2008. Application of nontraditional stable-isotope systems to the study of sources and fate of metals in the environment. Environ. Sci. Technol. 42 (3), 655–664. https://doi.org/10.1021/es0870855

Whitworth, P., Aldred, N., Reynolds, K.J., Plummer, J., Duke, P.W., Clare, A.S., 2022. Importance of duration, duty-cycling and thresholds for the implementation of ultraviolet C in marine biofouling control. Front. Mar. Sci. 8, 809011. https://doi.org/10.3389/fmars.2021.809011

Wiederhold, 2015. Metal stable isotope signatures as tracers in environmental geochemistry. Environ. Sci. Technol. 49, 2606−2624. https://doi.org/10.1021/es504683e

Wijesiri, B., Liu, A., He, B., Yang, B., Zhao, X., Ayoko, G., Goonetilleke, A., 2019. Behaviour of metals in an urban river and the pollution of estuarine environment. Water Res. 164, 114911. https://doi.org/10.1016/j.watres.2019.114911

Wijsman, J.W.M., Troost, K., Fang, J., Roncarati, A., 2019. Global Production of Marine Bivalves. Trends and Challenges, in: Smaal, A.C., Ferreira, J.G., Grant, J., Petersen, J.K., Strand, Ø. (Eds.), Goods and Services of Marine Bivalves. Springer International Publishing, Cham, pp. 7–26. https://doi.org/10.1007/978-3-319-96776-9_2

World Shipping Council (WSC), 2019. https://www.worldshipping.org/top-50-ports

Wu, P.C., Huang, K.F., 2021. Tracing local sources and long-range transport of PM10 in central

754 Taiwan by using chemical characteristics and Pb isotope ratios. Sci. Rep. 11, 7593.
755 https://doi.org/10.1038/s41598-021-87051-y

756 Xue, J., Lee, C., Wakeham, S.G., Armstrong, R.A., 2011. Using principal components analysis
757 (PCA) with cluster analysis to study the organic geochemistry of sinking particles in the ocean.
758 Org. Geochem. 42, 356–367. https://doi.org/10.1016/j.orggeochem.2011.01.012

759 Yin, N.H., Sivry, Y., Benedetti, M.F., Lens, P.N.L., van Hullebusch, E.D., 2016. Application of
760 Zn isotopes in environmental impact assessment of Zn–Pb metallurgical industries: A mini
761 review. Appl. Geochem. 64, 128–135. https://doi.org/10.1016/j.apgeochem.2015.09.016

762 Ytreberg, E., Bighiu, M.A., Lundgren, L., Eklund, B., 2016. XRF measurements of tin, copper
763 and zinc in antifouling paints coated on leisure boats. Environ. Pollut. 213, 594–599.
764 https://doi.org/10.1016/j.envpol.2016.03.029

765 Ytreberg, E., Lagerström, M., Nöu, S., Wiklund, A.K.E., 2021. Environmental risk assessment
766 of using antifouling paints on pleasure crafts in European Union waters. J. Environ. Manage.
767 281, 111846. https://doi.org/10.1016/j.jenvman.2020.111846

768 Yu, D., Wang, J., Wang, Y., Du, X., Li, G., Li, B., 2021. Identifying the source of heavy metal
769 pollution and apportionment in agricultural soils impacted by different smelters in China by
770 the positive matrix factorization model and the Pb isotope ratio method. Sustainability, 13,
771 6526. https://doi.org/10.3390/su13126526

772 Zhang, R., Cao, J., Tang, Y., Arimoto, R., Shen, Z., Wu, F., Han, W., Wang, G., Zhang, J., Li,
773 G., 2014. Elemental profiles and signatures of fugitive dusts from Chinese deserts. Sci. Total
774 Environ. 472, 1121-1129. https://doi.org/10.1016/j.scitotenv.2013.11.011

775 Zhu, Z., Sun, G., Bi, X., Li, Z., Yu, G., 2013. Identification of trace metal pollution in urban
776 dust from kindergartens using magnetic, geochemical and lead isotopic analyses. Atmos.
777 Environ. 77, 9–15. http://dx.doi.org/10.1016/j.atmosenv.2013.04.053

778

[List of Figures]

[List of Tables]

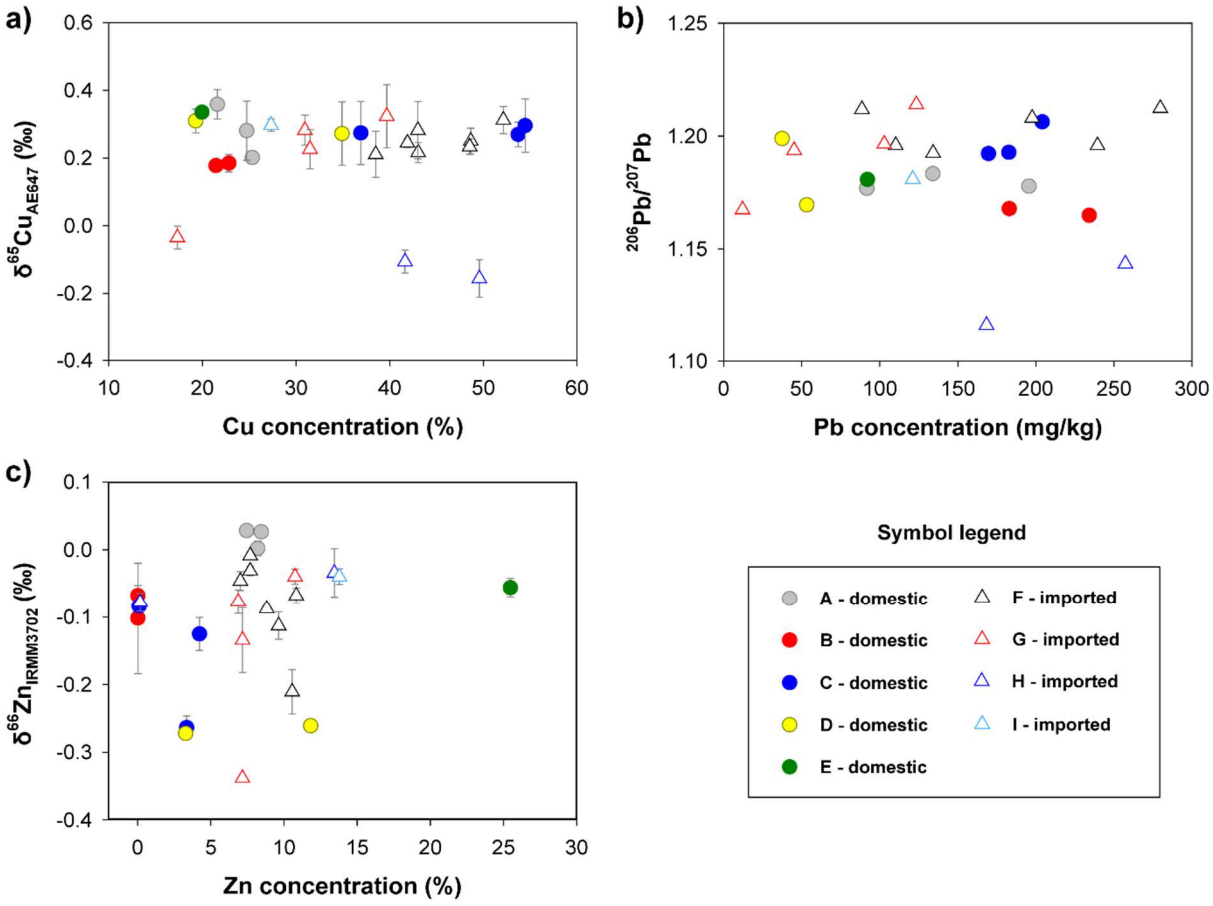

798

799 **Fig. 1**. Relationships observed in APs between Cu, Zn, and Pb concentrations and their isotopic
800 compositions. The error bars represent two standard deviations (2sd).

801

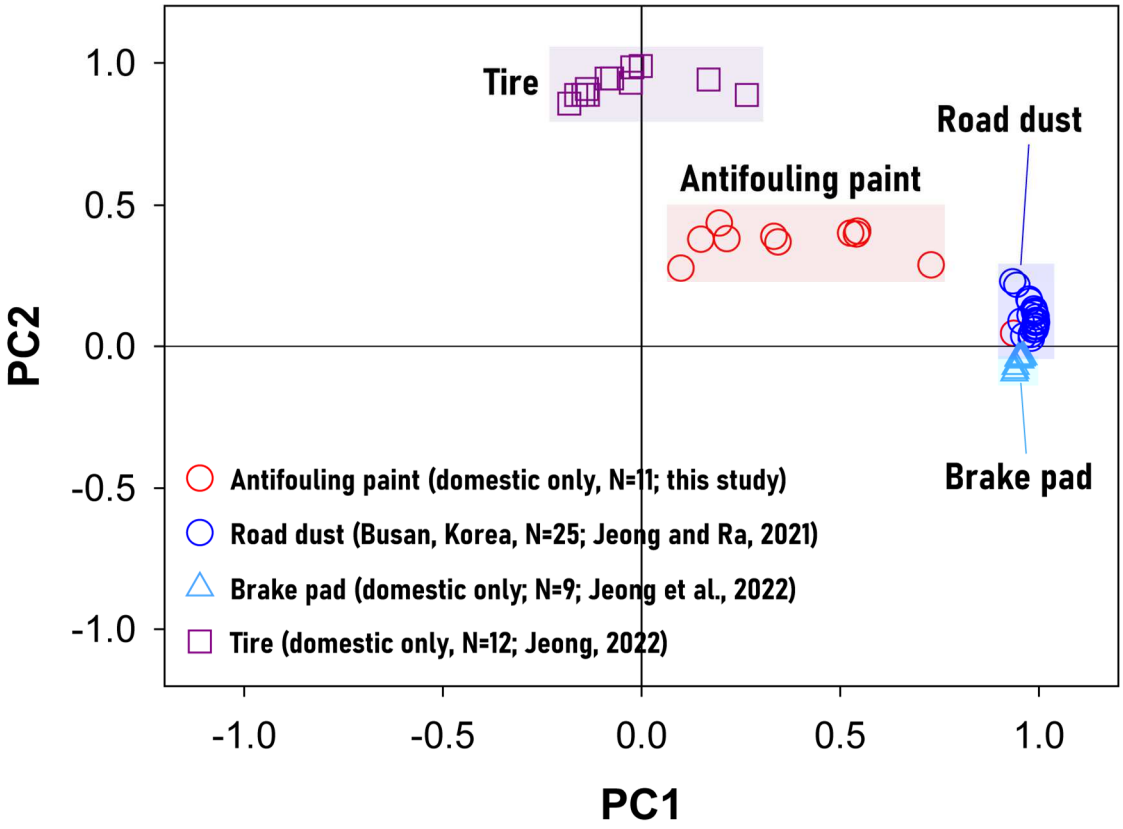

802

803 **Fig. 2.** Principal component analysis (PCA) results of metal concentrations and isotopic
804 compositions (Cu, Zn, and Pb) in antifouling paints, road dust, tires, and brake pads.

805

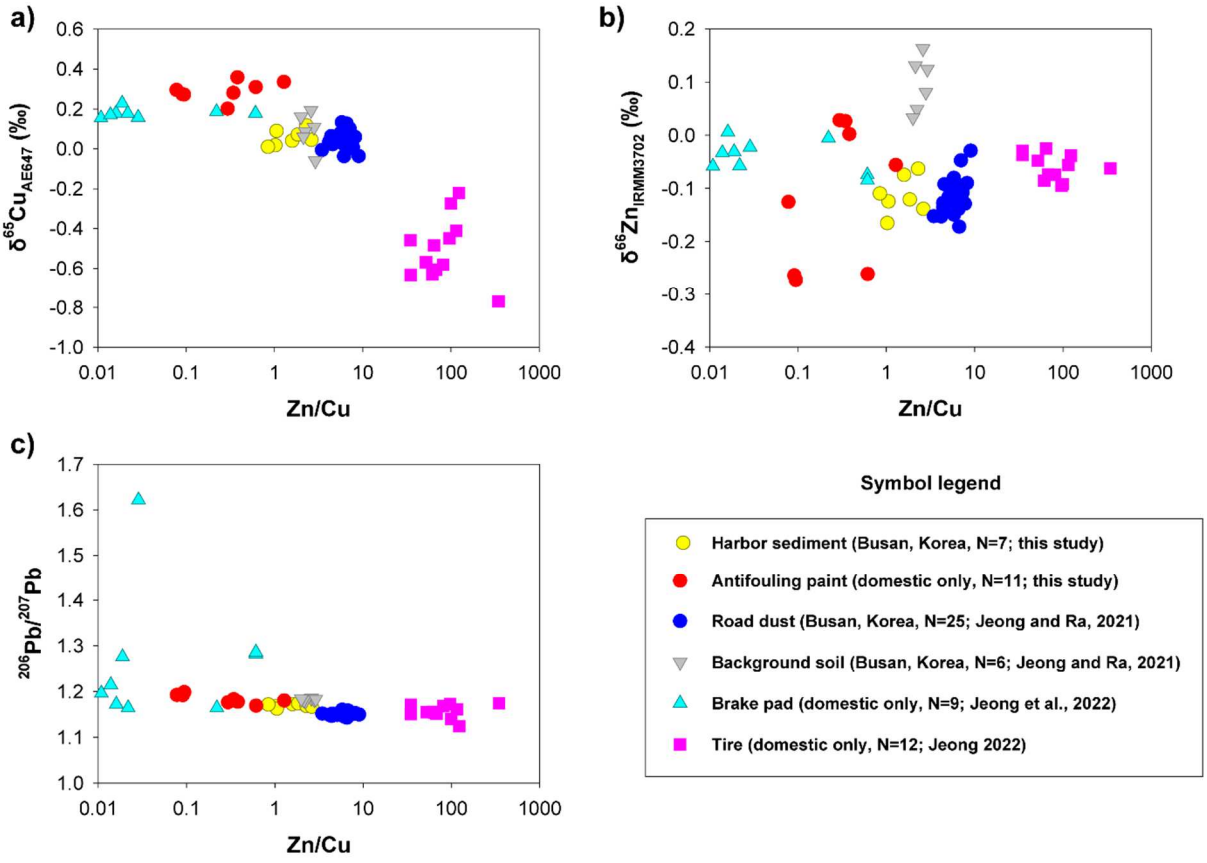

806

807 **Fig. 3**. Relationship between Zn/Cu ratios and isotopic compositions of Cu, Zn, and Pb in this
808 study.

809

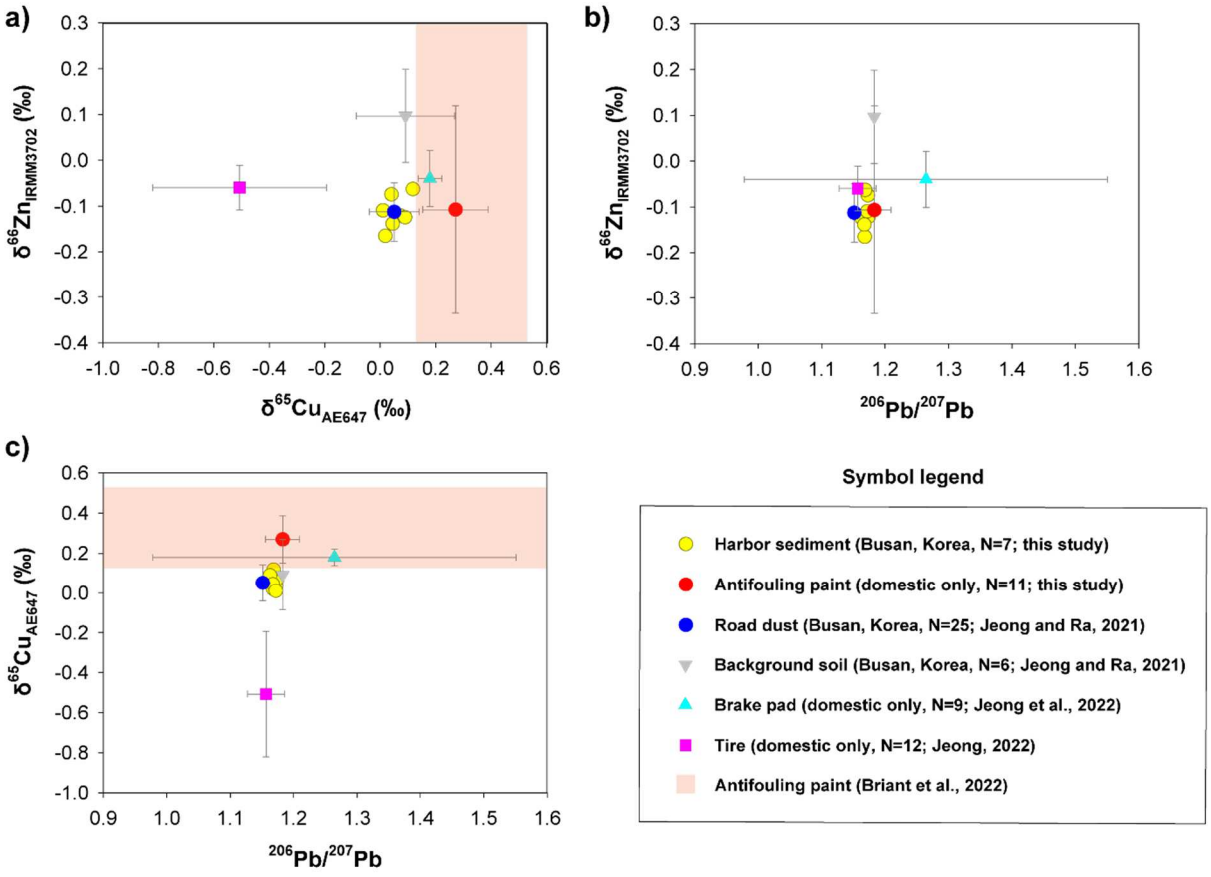

Fig. 4. Comparison between Korean harbor sediments and various pollution sources including APs using these and previously published Cu, Zn, and Pb isotopic compositions.

814 **Table 1**. Cu and Zn isotopic compositions of in-house standard solutions and reference
815 materials in this study with previously reported values.

	$\delta^{65}Cu_{AE647}$ (‰)	2sd	n	$\delta^{66}Zn_{IRMM3702}$ (‰)	2sd	n	References
ERM-AE633	–0.21	0.03	8				This study
Kanto Cu	0.12	0.01	8				This study
IRMM-651				–11.59	0.01	4	This study
Kanto Zn				–0.07	0.02	5	This study
BHVO-2	–0.08	0.03	3	–0.05	0.09	3	This study
BHVO-2				0.00	0.12		Sossi et al., 2015
BHVO-2	–0.08	0.10					Wang et al., 2020
BHVO-2	–0.06	0.16	4	–0.07	0.14	4	Jeong et al., 2021

816

817

Table 2. Comparison of mean, and standard deviation values for metal concentrations in antifouling paints used in Korea.

		Al	Fe	Ti	Mn	V	Cr	Co	Ni	Cu	Zn	As	Mo	Cd	Sn	Sb	Pb
	(unit)	%	%	%	mg/kg	mg/kg	mg/kg	mg/kg	mg/kg	%	%	mg/kg	mg/kg	mg/kg	mg/kg	mg/kg	mg/kg
Domestic antifouling paint makers (n=11)																	
A (n=3)	mean	0.16	2.93	3.49	29.2	0.91	59.1	0.77	41.7	23.87	8.03	1.41	2.62	0.65	212.7	5.50	140.3
	std	0.09	5.03	3.32	44.7	0.54	21.7	0.73	19.6	2.00	0.52	1.05	0.89	0.33	47.2	4.17	52.2
B (n=2)	mean	0.54	0.14	0.65	79.0	1.53	87.6	4.65	11.0	22.14	0.02	0.55	1.23	0.13	288.6	5.91	208.5
	std	0.06	0.00	0.71	10.8	0.40	20.5	1.54	0.02	0.97	0.00	0.03	1.04	0.00	8.4	0.56	36.2
C (n=3)	mean	0.19	0.97	0.76	21.1	6.01	57.8	1.85	211.5	48.35	2.56	1.94	5.65	1.97	638.3	6.33	185.4
	std	0.03	1.57	1.23	21.2	9.63	19.3	1.36	94.1	9.92	2.17	1.14	2.97	1.32	199.4	1.66	17.4
D (n=2)	mean	0.20	2.15	1.98	91.8	4.70	8.5	2.84	37.0	27.09	7.55	8.25	4.70	0.74	400.9	5.75	45.3
	std	0.05	2.91	2.76	62.4	4.12	4.0	3.21	9.4	11.04	6.04	9.53	2.48	0.42	266.0	5.85	11.1
E (n=1)	mean	0.11	5.39	0.01	22.8	1.39	26.1	0.95	57.1	19.95	25.46	1.97	2.73	0.56	190.5	2.93	92.1
Domestic	**mean**	**0.24**	**1.97**	**1.64**	**46.8**	**3.15**	**51.7**	**2.16**	**83.0**	**30.46**	**6.58**	**2.69**	**3.58**	**0.93**	**374.8**	**5.61**	**143.4**
	min	0.07	0.03	0.001	2.8	0.44	5.7	0.31	10.9	19.28	0.01	0.53	0.50	0.13	162.1	1.61	37.5
	max	0.58	8.74	6.62	135.9	17.13	102.1	5.74	318.2	54.44	25.46	14.99	8.99	3.49	851.5	10.11	234.1
	std	0.16	2.97	2.25	43.0	5.06	30.6	1.96	94.1	13.00	7.39	4.17	2.37	0.94	221.8	2.89	65.7
Imported antifouling paint makers (n=14)																	
F (n=7)	mean	0.23	0.45	1.66	9.0	1.06	30.3	0.78	91.5	45.10	8.89	1.30	2.69	1.14	396.3	4.88	195.7
	std	0.08	1.04	3.35	7.3	0.54	22.3	0.43	71.4	4.77	1.50	1.27	1.85	0.38	181.0	1.65	88.6
G (n=4)	mean	0.17	2.40	2.96	27.7	2.08	29.5	1.17	83.5	29.86	7.99	1.23	5.37	1.16	248.9	2.74	70.9
	std	0.10	3.03	4.15	27.2	1.96	28.2	0.99	57.1	9.26	1.85	0.79	5.21	0.97	203.1	1.81	51.3
H (n=2)	mean	0.06	0.88	0.18	10.4	0.40	11.0	1.21	30.8	45.59	6.81	7.23	3.95	10.10	127.4	3.45	212.8
	std	0.01	1.23	0.21	11.4	0.22	1.5	0.29	9.7	5.61	9.38	7.04	2.33	11.92	10.2	2.13	62.9
I (n=1)	mean	0.86	6.22	0.01	110.7	7.34	36.3	1.03	88.8	27.32	13.77	16.78	3.03	1.53	424.3	11.79	121.1
Imported	**mean**	**0.23**	**1.48**	**1.70**	**21.8**	**1.71**	**27.7**	**0.97**	**80.3**	**39.54**	**8.68**	**3.23**	**3.66**	**2.45**	**317.8**	**4.56**	**157.1**
	min	0.06	0.01	0.002	2.35	0.24	0.49	0.15	1.7	17.33	0.17	0.36	0.36	0.42	3.4	0.05	12.1
	max	0.86	6.35	9.13	110.66	7.34	76.32	2.39	235.91	52.12	13.77	16.78	12.24	18.52	755.4	11.79	320.2
	std	0.20	2.31	3.20	30.5	2.00	21.6	0.60	59.7	9.76	3.36	4.95	3.12	4.66	189.4	2.77	90.6
Harbor sediments (n=7)																	
Busan harbor sediment	**mean**	**8.01**	**4.06**	**0.40**	**515.9**	**90.55**	**74.1**	**11.81**	**27.9**	**196.2**[a]	**280.8**[a]	**11.28**	**1.62**	**0.36**	**7.1**	**1.37**	**60.1**
	min	6.83	3.20	0.34	473.2	69.05	55.9	8.07	17.2	115.1[a]	194.6[a]	9.78	0.92	0.17	4.7	1.02	41.6
	max	8.71	4.65	0.45	576.0	107.25	90.9	13.95	33.6	288.3[a]	464.7[a]	13.90	3.30	0.72	11.4	1.91	90.4
	std	0.59	0.48	0.04	47.0	11.90	11.3	1.97	5.4	77.9[a]	87.0[a]	1.47	0.80	0.19	2.8	0.35	20.9

[a]unit: mg/kg

820 **Table 3.** Comparison of mean, and standard deviation values for Cu, Zn, and Pb isotopic
821 composition of the present study.

		$\delta^{65}Cu_{AE647}$	$\delta^{66}Zn_{IRMM3702}$	$^{206}Pb/^{204}Pb$	$^{207}Pb/^{204}Pb$	$^{208}Pb/^{204}Pb$	$^{208}Pb/^{206}Pb$	$^{206}Pb/^{207}Pb$
	(unit)	‰	‰					
Domestic antifouling paint makers (n=11)								
A (n=3)	mean	0.28	0.02	18.4329	15.6298	38.1938	2.0720	1.1794
	std	0.08	0.01	0.0604	0.0052	0.0455	0.0043	0.0035
B (n=2)	mean	0.18	–0.08	18.2198	15.6207	38.0499	2.0884	1.1664
	std	0.005	0.02	0.0359	0.0024	0.0301	0.0024	0.0021
C (n=3)	mean	0.28	–0.16	18.7412	15.6550	38.4026	2.0492	1.1971
	std	0.01	0.09	0.1401	0.0128	0.1053	0.0097	0.0080
D (n=2)	mean	0.29	–0.27	18.5232	15.6412	38.2786	2.0668	1.1842
	std	0.03	0.01	0.3606	0.0309	0.1839	0.0304	0.0208
E (n=1)	mean	0.34	–0.06	18.4594	15.6333	38.1801	2.0683	1.1808
Domestic	**mean**	**0.27**	**–0.11**	**18.4971**	**15.6374**	**38.2387**	**2.0675**	**1.1829**
	min	0.18	–0.27	18.1944	15.6190	38.0286	2.0380	1.1649
	max	0.36	0.03	18.9027	15.6693	38.5242	2.0901	1.2063
	std	0.06	0.11	0.2292	0.0175	0.1502	0.0176	0.0134
Imported antifouling paint makers (n=14)								
F (n=7)	mean	0.25	–0.08	18.8081	15.6621	38.4439	2.0441	1.2009
	std	0.04	0.07	0.1730	0.0192	0.1382	0.0127	0.0096
G (n=4)	mean	0.20	–0.15	18.6768	15.6560	38.3278	2.0525	1.1929
	std	0.16	0.13	0.3279	0.0234	0.2223	0.0243	0.0192
H (n=2)	mean	–0.13	–0.06	17.5905	15.5718	37.4421	2.1288	1.1296
	std	0.04	0.03	0.3290	0.0219	0.3036	0.0226	0.0195
I (n=1)	mean	0.30	–0.04	18.4462	15.6364	38.2379	2.0707	1.1810
Imported	**mean**	**0.18**	**–0.09**	**18.5722**	**15.6456**	**38.2529**	**2.0605**	**1.1870**
	min	–0.16	–0.34	17.3579	15.5563	37.2274	2.0261	1.1158
	max	0.32	–0.01	19.0440	15.6864	38.6538	2.1447	1.2140
	std	0.16	0.09	0.4790	0.0368	0.3871	0.0338	0.0279
Harbor sediments (n=7)								
Busan harbor sediment	**mean**	**0.06**	**–0.11**	**18.2739**	**15.6263**	**38.3801**	**2.1003**	**1.1694**
	min	0.01	–0.17	18.1681	15.6166	38.2353	2.0977	1.1630
	max	0.12	–0.06	18.3619	15.6347	38.5190	2.1046	1.1744
	std	0.04	0.04	0.0677	0.0068	0.1185	0.0025	0.0039

822

823

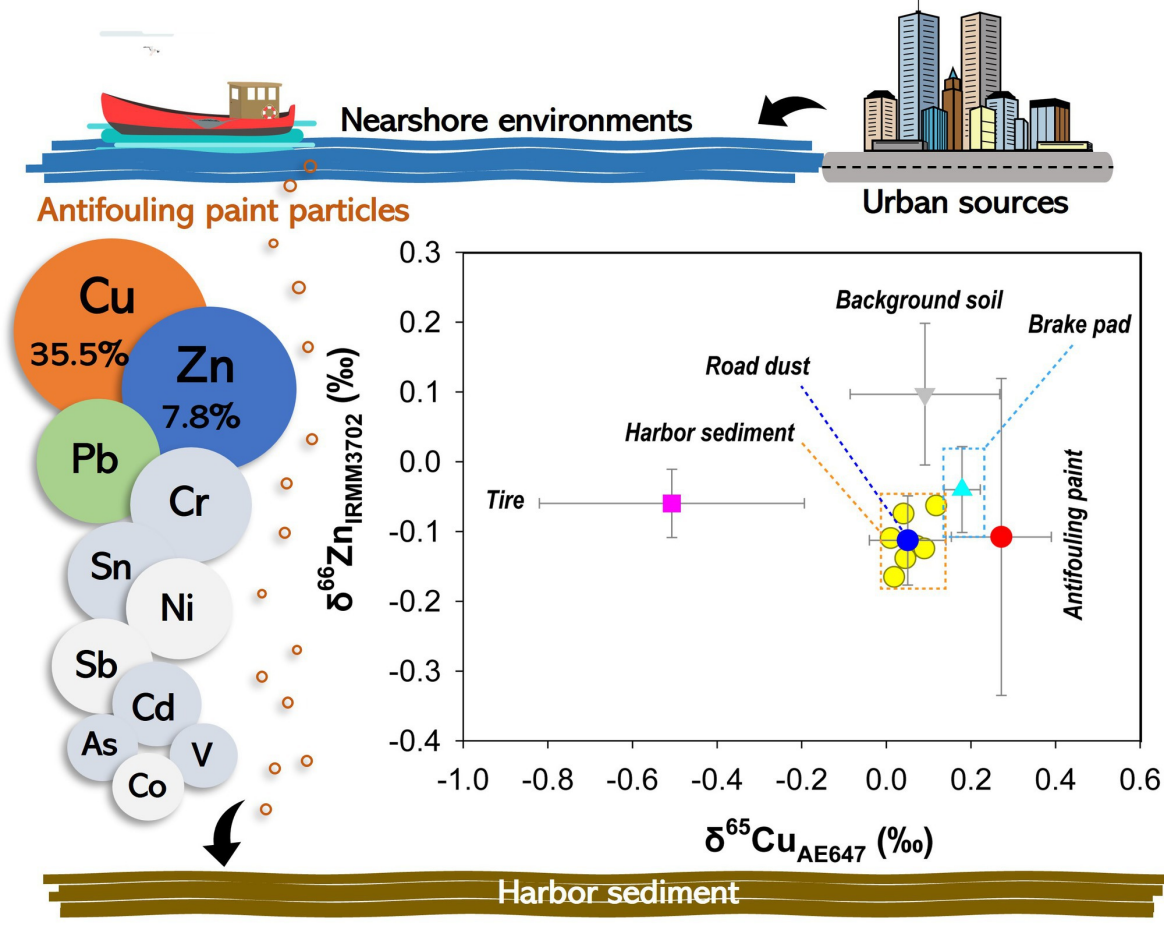
Nearshore environments
Urban sources
Antifouling paint particles
Cu
35.5%
Zn
7.8%
Pb
Cr
Sn
Ni
Sb
Cd
As
V
Co
Background soil
Brake pad
Road dust
Harbor sediment
Tire
Antifouling paint
δ66ZnIRMM3702 (‰)
δ65CuAE647 (‰)
0.3
0.2
0.1
0.0
-0.1
-0.2
-0.3
-0.4
-1.0
-0.8
-0.6
-0.4
-0.2
0.0
0.2
0.4
0.6
Harbor sediment